

Original Paper

Geohydrodynamic Parameters and Their Implications on the Coastal Conservation: A Case Study of Abak Local Government Area (LGA), Akwa Ibom State, Southern Nigeria

U. E. Uwa,¹ G. T. Akpabio,¹ and N. J. George^{2,3}

Received 1 April 2018; accepted 27 June 2018
Published online: 4 July 2018

A total of 14 vertical electrical soundings using Schlumberger electrode configuration and the complementary laboratory analysis of aquifer samples were carried out in the Abak Local Government Area of Akwa Ibom State, the coastal region of Nigeria. The study focused on the estimation of geohydrodynamic parameters of the frequently exploited aquifers and the implication of hydrodynamic parameters on the lithostratigraphy and the anticipated exposure of the assessed geologic formation at the shorelines. These parameters were porosity (ϕ), tortuosity (τ), formation factor (F), aquifer water formation resistivity (R_w) and coefficient of permeability/hydraulic conductivity (K). Computation of the effective porosities from the aquifer cuttings was carried out using wet weight–dry weight technique and petrophysical techniques. The F values were computed using the aquifer formation bulk resistivity measured from field 1-D resistivity data analysis, whose interpretation was constrained by nearby borehole information. The formation pore water resistivities were estimated from the laboratory using electrical resistivity metre. The Win RESIST software program was used in interpreting the field data electronically. The results of interpretation gave the primary parameters of saturated and unsaturated units of the coastal regions used in this work. The area generally shows seemingly high porosity with high coefficient of permeability. The primary and secondary parameters have been contoured to model their distributions. Besides, some functional relations have been realized through regression analyses. The contour distribution of the geohydrodynamic parameters indicates the vulnerability of the water repositories to contaminations as well as the vulnerability of the shoreline to waterborne erosion. The seemingly high effective porosity in the compliant laboratory and calculated values indicate that the coastal region is neither lithified nor compacted/consolidated. This signals the possibility of the formation to be easily eroded, weathered or flooded where these units are exposed to water current. With these revelations, the shorelines could be properly managed and conserved by geotechnically reinforcing with hard and water-resistant concrete that can protect the vulnerable and erosion-prone porous sediments.

KEY WORDS: Geohydrodynamic parameters, Coastal management, Coastal shorelines, Abak, VES.

¹Department of Physics, University of Uyo, Uyo, Nigeria.

²Department of Physics, Akwa Ibom State University, Mkpata Enin, Nigeria.

³To whom correspondence should be addressed; e-mail: nyaknojimmy@gmail.com

INTRODUCTION

Inasmuch as groundwater has a natural protection against pollution, due to the top layers, which

cover the hydrogeological repositories, it requires minor water treatment. This makes groundwater a more preferable source of water supply when compared to surface water (George et al. 2018). Nowadays, the need for improved accuracy in global groundwater resource evaluation has led to a rapid growth in groundwater management and conservation. These geohydrodynamic parameters are porosity (ϕ), tortuosity (τ), coefficient of permeability/hydraulic conductivity (K) and formation resistivity factor (F). Porosity is the ratio of space taken up by pores in a soil or rock to the total volume of the soil/rock. In saturated layers (layers under the water level characterized by interstices, which are inundated or filled with water and air), the pore water content of a geologic formation is proportional to its porosity. Generally, porosity (ϕ) of sediments can be classified into absolute porosity and effective porosity (Pettijohn and Potter 1972; Gurunadha Roa et al. 2011; Obianwu et al. 2011). Effective porosity results when void spaces are interconnected and the pore–matrix system is able to transmit fluids. Absolute porosity is the fraction of void volumes with respect to the bulk volume, regardless of pore connections in which the pore–matrix system is not able to transmit water/fluid (Folk 1966). Total porosity encompasses the water in clay that has dead-end pores. Fine-grained clastic sediments can produce enhanced porosity compared to coarse-grained sediments of clastic origin. This is because pore communications/contacts among fine grains gradually increase, leading to decrease in packing of geological formation system (George et al. 2014). Gratan and Fraser (1935) in their studies of pore–grain arrangements formulated mathematical porosity models for arrangement of unique spheres. Formation of loosest stable arrangements with equal spheres whose centers form space lattice of rectangular shape or cubic packing result when contact is made with six nearby spheres and the fractional porosity value was determined by Gratan and Fraser (1935) to be maximum with numerical value 0.48. However, in the packing of densest formation, whose center of spheres form a rhombohedral shape, each of the spheres is connected with 12 nearby spherical formation. Gratan and Fraser (1935) also considered the porosity in this arrangement to be minimum, with a numerical value of 0.26. These illustrations suggest that highly tight clastic sediments have lower porosity while loosely tight sediments have higher porosity. Beyond this established fact, the arrangement of spheres and the shape of packing, uniformity, sorting of grains and shapes among other factors also play

dominant role in the porosity values of a geologic unit. Because grains of sediments appear to arrange in edge–edge or edge–face directions in plate-like shape, porosity increases as the curve-shaped deposited grains predominate. Argillites suffer more than hard grains from arenaceous materials due to increase in confining stress in the loading sediments. As the stress of confinement increases, a significant change in the porosity of sedimentary system is noticeable. The study of Kezdi (1974) suggested that values of porosity spanning from 0.38 to 0.55 correspond to loose arenaceous materials, sand and silts while the range of 0.18–0.40 corresponds to the same clastic sediments in the dense form. In the same vein, Kezdi (1974) proposed a porosity range of soft argillites to be 0.45–0.70 while 0.30–0.40 was proposed for hard argillites.

Ground-based and laboratory measurements can enable the estimation of formation factor (F), which gives information related to porosity of reservoirs, water repositories and even in geological foundations. This information gives the electrical attributes of formation lithologies, formation conductivity, viscosity, pore water temperature, pore water saturation, clay content, specific surface and electric surface conductance referred to as mechanism of charge fixation at the fluid–solid interface. Other realizable information from F includes prediction of pore-shaped system, permeability, pore and pore channel (tortuosity), cation exchange capacity. Formation factor links with the extent of mineralogy, cementation, consolidation and compaction, which determine the ease of weathering of formation in the region of less pressure such as coastal shorelines. The formation factor is defined as:

$$F = \frac{\rho_b}{\rho_w} = F = \frac{a}{\phi^m} \quad (1)$$

where ρ_b and ρ_w stand for bulk and water resistivity, respectively. For clastic sediments and rock of sedimentary origin, Archie (1942) and Winsauer et al. (1952) theorized equations referred to as Archie–Winsauer equations. These expressions in Eqs. 1 and 2 (alternative of Eq. 1) demonstrate the correlation between F and fractional porosity (ϕ) in relation to pore geometry factor a and Archie cementation factor m , thus:

$$\log a = \log F + m \log \phi \quad \text{or} \quad m = - \left\{ \frac{\log F - \log a}{\log \phi} \right\} \quad (2)$$

The value of m exhibits a spectrum of variations among media, samples, formations and intervals. Atkins Jr. and Smith (1961) opined that the value of m considerably varies from medium to high due to shape–pore grain variations. Ehrlich et al. (1991) in their own observation concluded that values of m changes widely and continuously in borehole due to changes in surfaces of deposition. The cementation factor (m) depends on many factors such as grains, shape and many other factors affecting formation factors mentioned earlier. More angular than spherical grains connotes higher values of m . Higher angularity gives rise to elevated content of argillites and heterogeneous composition of clastic sediments, which lead to elevated m . Heterogeneity of pore system leads to changes in m . Increase in fracturing through change of pore system reduces the value of m according to Aguilera (1976), while increase in pores of formation leads to increase in m . When a rock is compressed, sudden changes occur in pore and shape system of grains, thereby leading to high ease of deformation. The deformation of geological sediment/rock is associated with aggregation of thermal shift of grains, constriction of pore, elevation of resistivity and angularity as well as high cementation factor. The summary of m as indicated by Keller (1982) entailed that m depends on porosity, lithology, age of formation, cementation and compaction of formation.

According to Archie (1942), Wyllie and Rose (1950) and Wyllie and Gregory (1953), m can vary between 1 and ∞ . However, in practice, it falls within the range of $1.3 < m \leq 3.0$. The tortuosity factor/pore geometry factor indicates the geometry of pores in porous media. From literatures, pore geometry factor increases adversely with decrease in the age of geologic formation, consolidation and compaction. According to Winsauer et al. (1952), the equation for sandstones (consolidated) is:

$$F = \frac{a}{\phi^m} = \frac{0.52}{\phi^{2.15}} \quad (3)$$

In sediments with inter-granular porosity, the value of a can be unity (Keller and Frischknecht 1966).

Tortuosity (τ) is a dynamic parameter which characterizes the geohydrodynamic mechanism of a porous medium by description of the shape of flow of electric and hydraulic quantities as well as the complexity of the channel network of porous media. Tortuosity is a numerical value that quantifies the degree of departure of a porous system from being

composed of a bundle of straight capillary flow tubes. According to Bear (1972), it is also the ratio of mean length of all particle path lines crossing a given cross section during a unit period to width of the sample. Different methods abound for determining tortuosity. These include theoretically mathematical derivation of models (Owen 1952; Towel 1962), and numerical method explores mathematical relations of tortuosity and other geoelectrohydraulic parameters (George et al. 2015a, b, 2017a). According to Carman (1937, 1938, 1956), experiment on conductivity and diffusion can be explored to determine tortuosity. Moreover, the techniques of ion transit times (Winsauer et al. 1952) and capillary pressure curve of pore distribution (Faris et al. 1954) can be used to determine tortuosity in a given porous medium. By derivation, tortuosity τ can be obtained by finding the square root of the product of formation resistivity factor F and fractional porosity ϕ of a given unconsolidated heterogeneous porous medium, thus:

$$\tau = (F\phi)^{\frac{1}{2}} \quad (4)$$

Non-disorderliness of tortuous fluid flow was demonstrated by Carman (1937) in hydraulic radius R_h given in Eq. 5. The flow of fluid traverses its way through the path of a porous medium by navigating its direction from one point to another unhindered. The R_h is derived by finding the ratio of porosity to specific surface area S_s measured in square meter:

$$R_h = \frac{\phi}{S_s} \quad (5)$$

Hydraulic conductivity (coefficient of permeability), (K), is linked to laboratory-measured porosity ϕ_{lab} and can be estimated using the Kozeny–Carman–Bear’s equation given as:

$$K = \left[\frac{g \cdot \sigma_w}{\mu_d} \right] \cdot \left[\frac{d^2 m}{180} \right] \cdot \left[\frac{\phi_{lab}^3}{(1 - \phi_{lab})^2} \right] \quad (6)$$

where g is gravitational acceleration, σ_w is water density (1000 kg/m^3), dm symbolizes the grain mean size of sand determined directly from micrometer screw gauge and μ_d symbolizes water dynamic viscosity (0.0014 kg/ms) of sandy formation (Fetters 1994; George et al. 2015a). This parameter is a very important geohydrodynamic tool that can be used to determine the flow of fluid through a formation and its associated damaging effect on the formation such

as coastal shorelines. Generally, in this context, permeability refers to the ease of a geologic formation to allow the flow of water current through it under the application of hydraulic pressure. Its coefficient is defined for a sample of geologic unit through the use of Darcy law in Eq. 7

$$\text{Coefficient permeability} = \frac{(\text{yield}/\text{section})}{\text{pressure gradient}} \quad (7)$$

In Eq. 7, yield is measured in m^3/s , and the section of the sample is expressed in m^2 . The difference in water pressure/sample length or pressure gradient is expressed in meter per meter (m/m). Hence, permeability coefficient is measured in m/s. The unit is suggestive of the speed of flow of fluid in a formation. The wearing/weathering of coastal shoreline can be dependent on the porosity, permeability tortuosity, the formation pore system and the type of geologic formation which determines the magnitude of these geohydrodynamic parameters.

LOCATION AND GEOLOGY OF THE AREA

The study area is located between longitudes $7^{\circ}43'E$ and $7^{\circ}49'E$ and latitudes $4^{\circ}25'N$ and $5^{\circ}25'N$. It is not centrally located in Akwa Ibom State. It is bounded in the north by Essien Udim, west by Etim Ekpo LGA, south by Ukanafun LGA and east by Uyo. This survey was arranged to cover some areas in the Abak LGA, Akwa Ibom State, Nigeria, a region surrounded by both fresh and saline water in the Niger Delta. The survey area is situated within a zone of climate with two noticeable seasons. The first is rainy season that begins from March to October, and the second is dry season that begins from November to February of every year (Evans et al. 2010; George et al. 2010). Practically, there seems to be no noticeable sharp boundary between these two seasons. The monthly average surface temperature varies from 5.5 to 6.5 °C compared to annual average temperature. The minimum daily mean temperature lies between 23 and 24 °C during July and August, and the maximum daily average surface temperature is between 28 and 30 °C during March (Igboekwe et al. 2004).

The study area lies within the arcuate deltaic depositional environment of the Niger Delta, southern Nigeria. The topmost unit of this region is

known as the coastal plain sands, also known as Benin Formation. This formation in the sedimentary basin is the youngest in the Delta. The Agbada Formation, which underlies the Benin Formation, is known to be laid down in a paralic brackish marine fluvial, coastal and fluvio-marine environment that consist of inter-bedded sands and shales. The coastal plain sands, which vary in thickness from 0 to 4.572 km, become more shaly with depth. This formation hosts the main hydrocarbon reservoirs of Nigeria (George 2006). The most remarkable structure in the Niger Delta is growth fault, which contributes to the formation of oil traps. The essential features of the Benin Formation have been reviewed by various authors. Kogbe (1989) described the Benin Formation as a composition of chiefly continental sands, which show variable grain sizes and intercalations of shale and thickness that exceeds 1.829 km (6000 ft). Mbipom et al. (1996) opined that the high permeability of the Benin Formation, the overlaying lateritic and weathered top layer of this formation as well as the underlying clay–shale sequence provide the hydrologic conditions favoring aquifer formation (George et al. 2016). The geologic map of the study area shows that the area is underlain by coastal plain sands. This Benin Formation has sediments and sedimentary rocks formed by terrestrial or marine deposits. The formation is mainly unconsolidated or lithified with no relation to geologic age. The highly permeable nature of this sedimentary formation exposes the shoreline in the coast to excessive erosion.

METHODOLOGY AND FIELD STUDIES

Due to the dependence of earth resistivity on some geologic parameters, ground-based electrical study and laboratory analysis of soil samples have been carried out. The electrical resistivity surveys were carried out in 14 stations during 2015–2016, across the study area. An ABEM terrameter SAS 1000 model and its accessories were used in the survey. The extension of current electrode spacing (AB) was limited by infrastructures and settlement conditions of the area. Hence, values of AB varied from station to station. This confined the locations of vertical electrical sounding (VES) points to the locations in Figure 1. Locations characterized by good access road/paths enabled the extension of AB from 500 to 1000 m, which comfortably allows

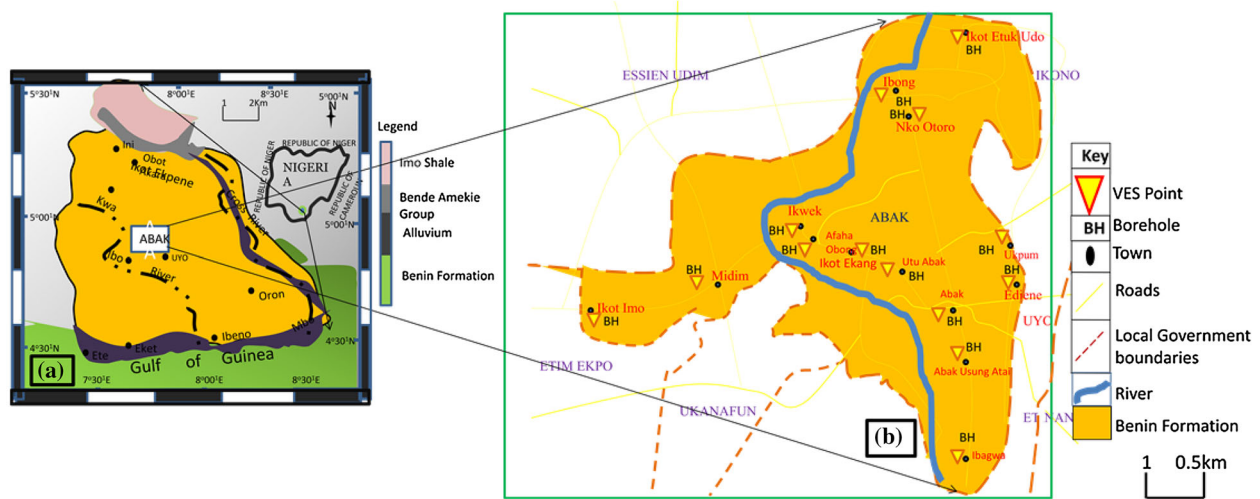


Figure 1. (a) Map of Akwa Ibom State showing the location and geology of the study area, (b) map of the Abak Local Government Area showing geology, VES station and boreholes.

sampling of depths above 200 m. The receiving (potential) electrode separation (MN) ranged from 0.5 m at AB = 2 m to 50 m at AB = 1000 m. As precautionary exercise, the potential electrode separations did not exceed one-fifth of current electrode separations (Gowd 2004). During the rainy season, the data quality was unique whereas during dry season contact resistance was avoided by saturating the electrode stations with water. This exercise also improved the soil–steel electrode contact and conductivity. The VES locations were sited in areas where there are geologically logged boreholes with drill cuttings in order to constrain the VES data with geology. Many of the VES stations were positioned in such a way that water boreholes are adjacent to them, whereas in some locations, water boreholes were placed in positions where there is no possibility for laying VES cables. In such scenarios, VES stations were about 100–150 m away from water borehole locations. The collection of water sample and in situ measurement of water electrical resistivity were carried out using resistivity meter in all the water boreholes used in this survey.

In order to have anomaly that is associated with geologic origin, electrodes were generally planted so that at least two-thirds of their lengths went under the ground surface at any instance. Also associated with electrode is the fact that where a sharp change in the measured resistance was observed, replanting of the electrode (current electrodes) at other points

within their vicinity sometimes yielded a more reliable result. During the VES measurements, the terrameter self-check was very effective as it warned the operator of any disconnection of either the potential or the current electrodes. Nevertheless, except where the operator is able to notice, the terrameter gave no warning (beeper signal) when the terminal of P₁ and P₂ or C₁ and C₂ were, respectively, alternated. A trial showed that while alternation of C₁ and C₂ terminal did not seem to change an earlier result, alternation of P₁ and P₂ led to a sharp increase in resistance values. It therefore served a good field practice to ensure that proper connections were maintained throughout the duration of such sounding.

Components of argillaceous materials obtained from the coring operation were according to API (1960) and removed from the drill cutting by pre-washing with distilled water. The water samples were inserted in vacuum desiccators and a pressure of 0.3 mbar was used to evacuate them for duration of 60 min (Emerson 1969). The distilled sample of water, which was de-aerated, was poured into the desiccators carefully to cover the water sample. Traces of salt and other related soluble contaminants within the sample effused into the surrounding water by soaking all the samples for a period of 1 day. The clean samples were dried in a temperature-controlled oven at 105 °C for 16 h to ensure that the composition of the sample is not reversed (Emerson 1969; Galehouse 1971). The cored sam-

ples, which were oven-dried, were kept to cool in desiccator to ambient air temperature. The sample dry weight W_d was taken through the use of an electronic weighing balance for several times. After this, the average weight was calculated and recorded. The samples that were soaked for 18 h in water were boiled in a vacuum pressure of 0.3 mbar for half an hour. The sample wet weight W_w was taken several times to determine the average, which is believed to be reliable. Fractional values of effective porosity (ϕ) for the aquifer cuttings were estimated as:

$$\phi = \left(\frac{W_w - W_d}{v} \right) \quad (8)$$

where v is volume of samples. Detailed experimental procedures are available in API (1960), Emerson (1969) and Galehouse (1971).

The calculation of bulk resistivity from measured bulk resistance R_a was the first step in VES data analysis using the following equation:

$$\rho_a = \pi \frac{\left[\frac{AB}{2} \right]^2 - \left[\frac{MN}{2} \right]^2}{MN} \cdot R_a \quad (9)$$

Bulk resistivity ρ_a values for each of the current electrodes (AB) and potential electrodes (MN) separations were calculated in Ω m. The most compliant values of apparent resistance R_a were used, but sometimes, the mean apparent resistance for the selected cycles was used provided the standard error was not more than $\pm 0.05 \Omega$ or $m\Omega$ depending on the range used. The calculated values of Schlumberger apparent resistivity ρ_a were further cross-checked to ensure their correctness. For each electrode spacing (AB/2) on a bilogarithmic graph, VES curves were obtained and smoothed. The techniques used by Zohdy (1965), Zohdy et al. (1974), Ibuot et al. (2013), Ibanga and George (2016) for VES data processing were adopted for the reduction of earth models from VES data. The procedure for manual processing of VES data involved use of bilogarithmic graphs, for plotting of the calculated apparent resistivity. At times, the resulting noisy curve signatures were smoothed. According to Bhattacharya and Petra (1968), Akpan et al. (2009) and Chakravarthi et al. (2007), this was done to get rid of outliers caused by lateral heterogeneities that have no geological significance. Based on Orellana and Mooney (1966), the deployment of partial curve matching method, which employs master curves/charts, aided in the preliminary analysis of the data.

Thereafter, modeling of the VES data electronically was done using the Win RESIST software program. This was possible through the use of initially smoothed layer parameters obtained through manual analysis. The software program performed some calculations and generated theoretical data, which it compares with the field data for goodness of fit in the generation of the final models for resistivity, thickness and depth as shown in the typical VES curves model in Figures 2a and 3a. Due to inherent problems of equivalence and suppression, which make quantitative interpretation of VES data difficult, borehole data in Figure 2a and b were, according to Vanovermreen (1989), used in constraining all depths as they helped in minimizing the choice of layer models through the fixing of layer thickness and depths as the resistivity varies at point of inflections (Batayneh 2009).

The maxima and minima that were noticed on a smoothed VES curve were employed in half-space data inversion process. The goodness of fit revealed root-mean square error (RMSE) was due to the iterative performance of the software at each level. This iteration updates the input parameters based on the fitness between the theoretical and field data. In this analysis, the acceptable RMSE for achievable goodness of fit was 6%. The generated VES curves gave the initial geoelectric information which includes layer resistivity, depth and thickness.

RESULTS AND DISCUSSION

Based on the initial parameters obtained from sounding curves and laboratory analyses, geohydrodynamic parameters were estimated and are provided in Tables 1 and 2. The typical dominating groups of curves are represented in Figures 2a and 3a; these curve types are KH and AK, respectively. At other VES locations, other types of curves such as H, A and Q were realized. Generally, three to four geoelectric layers were identified in all the VES points (see Table 1). Table 1 shows the summary of the geoelectric computer-aided model for the study area. The table shows primary and significant parameters like formation resistivity, depth to bottom and thickness of layers, which are needed to compute the dynamic flow parameters of the aquifer units. The table also shows the number of layers penetrated by the current, the location names, location coordinates, mean elevation above sea level and curve types inferred in the study. The first layer

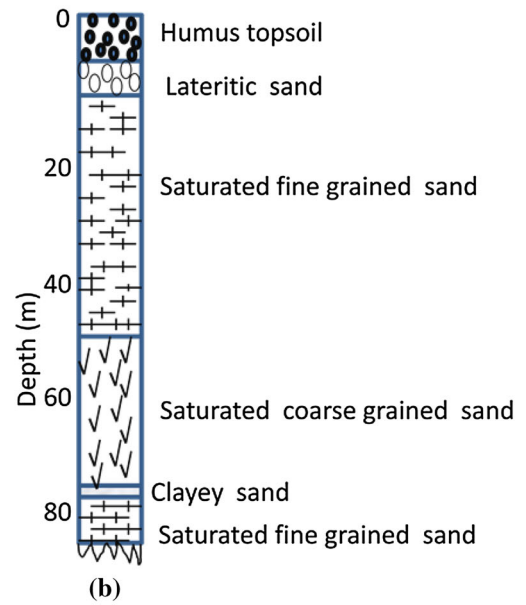
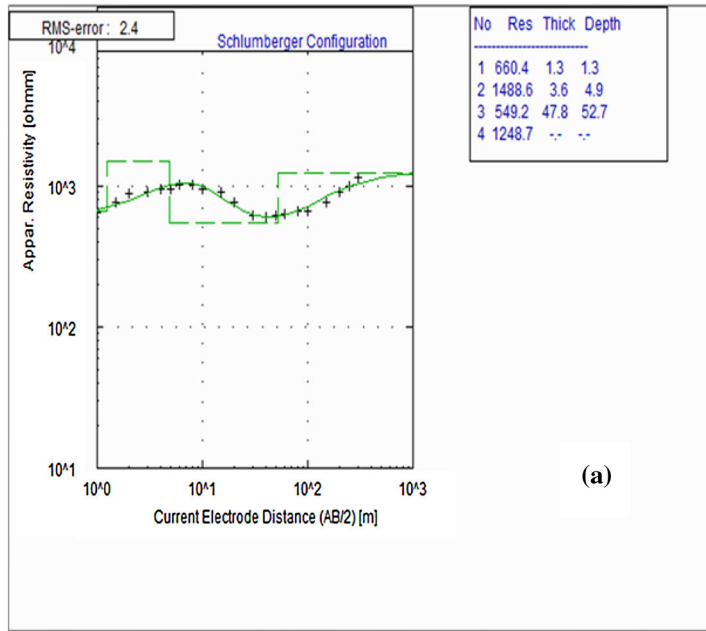


Figure 2. (a) Typical VES curve model obtained at VES 1 in Ikot Imo representing KH curve type. (b) Lithology log of a borehole near VES 1.

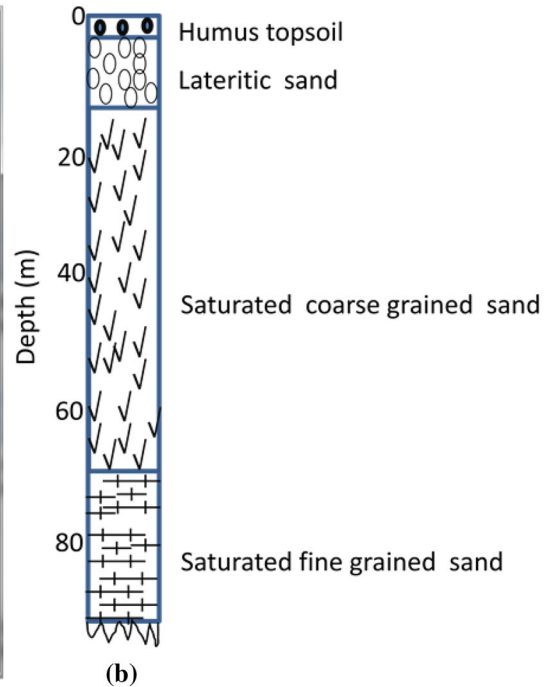
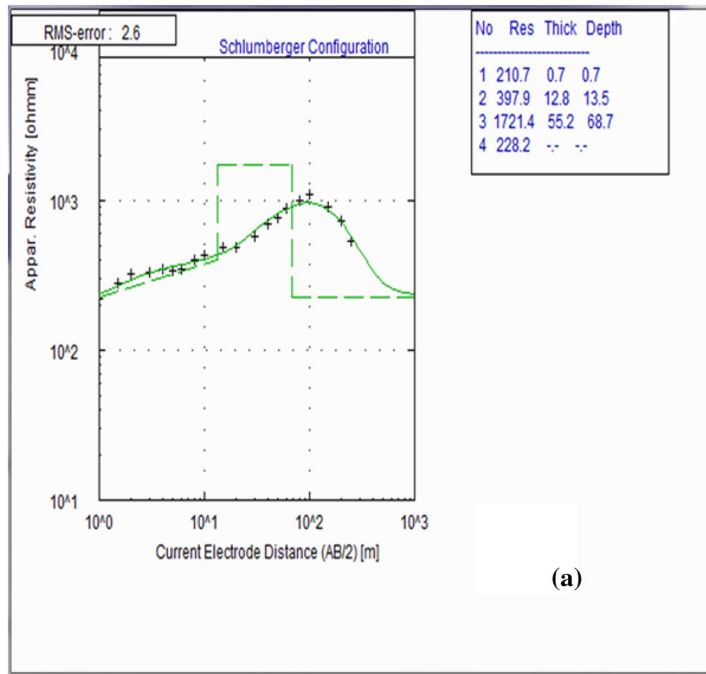


Figure 3. (a) Typical VES curve model obtained at VES 9 in Ikot Imo representing AK curve type. (b) Lithology log of a borehole near VES 9.

Table 1. Summary of results of geoelectric survey from computer modeling

VES no.	Location	Coordinate	Elevation (m)	Layer no.	Layer resistivity (Ω m)				Layer thickness (m)			Layer depth (m)			Curve type
					ρ_1	ρ_2	ρ_3	ρ_4	h_1	h_2	h_3	d_1	d_2	d_3	
1	Ikot Imo	5.0214N 7.7274E	20.0	4	660.4	1488.6	5492	1248.7	1.3	3.6	47.8	1.3	4.9	52.7	KH
2	Midim	5.0285N 7.7209E	16.0	3	554.2	362.2	1888.4	-	11.3	170.4	-	11.3	181.7	-	H
3	Ikwek	5.0335N 7.7509E	12.0	4	71.8	471.8	166.5	2585.3	0.5	6.3	43.3	0.5	6.8	50.1	KH
4	Ikot Ekang	5.0133N 7.7603E	10.0	3	206.8	181.1	751.8	-	0.9	108.9	-	0.9	109.8	-	H
5	Utu Abak	5.0059N 7.7688E	10.0	4	120.0	222.3	1945.6	62.3	4.2	2.0	68.1	4.2	6.2	74.3	AK
6	Ukpom	5.0201N 7.8176E	11.0	3	873.2	71.3	2332.5	-	5.1	81.1	-	5.1	86.2	-	H
7	Afaha Obong	5.0692N 7.7348E	12.0	4	892.4	2510.2	1661.8	1845.2	6.2	58.8	19.8	6.2	65.0	84.8	KH
8	Nko Otoro	5.0808N 7.7898E	15.0	4	115.8	577.7	1115.9	46.1	4.3	6.0	105.3	4.3	10.3	115.6	AK
9	Ibong	5.1038N 7.7883E	13.0	4	210.7	397.9	1721.4	228.2	0.7	12.8	55.2	0.7	13.5	68.7	AK
10	IkotEtuk Udo	5.1113N 7.7883E	14.0	4	205.8	750.3	52.6	68.8	2.9	11.8	68.2	2.9	14.7	82.9	KH
11	Ediene	4.9809N 7.8007E	13.0	3	102.6	735.5	1465.9	-	7.6	87.7	-	7.6	95.3	-	A
12	Abak	4.9831N 7.7875E	14.0	4	718.4	1844.9	1362.2	1446.8	0.5	1.6	38.9	0.5	2.1	41.0	KH
13	AbakUsung Atai	4.9344N 7.7999E	15.0	3	392.5	197.7	74.9	-	2.4	57.9	-	2.4	54.2	-	Q
14	Ibagwa Barracks	4.9019N 7.7978E	13.0	3	4023.3	1259.2	3428.8	-	11.3	83.0	-	11.3	94.3	-	H

Table 2. Summary of aquifer petrophysical parameters

VES no.	ρ_b (Ω m)	ρ_w (Ω m)	F	Φ_{lab}	Φ_{cal}	Residual	τ	K (m/s)	K (m/day)	h (m)	S (Ω^{-1})	T (Ω m ²)	Tr (m ² /day)	Lithologic description of sandy units
1	549.2	130.5	4.2	0.326	0.355	0.009	1.76	0.000357	30.855	52.7	0.095958	28,942.84	1626.0798	Gravelly
2	362.2	88.2	4.1	0.333	0.339	0.006	1.16	0.000389	33.589	170.4	0.470458	61,718.88	5722.0131	Medium
3	166.5	42.9	3.9	0.338	0.350	0.012	1.17	0.000413	35.648	43.3	0.26006	7209.45	1543.5484	Gravelly
4	181.1	50.5	3.6	0.344	0.365	0.021	1.14	0.000443	38.271	108.9	0.601325	19,721.79	4167.6741	Medium
5	1945.6	328.1	5.9	0.278	0.280	0.002	1.29	0.000193	16.675	68.1	0.035002	132,495.3	1135.5476	Medium
6	71.3	5.7	12.5	0.182	0.189	0.007	1.54	4.22E-05	3.6451	81.1	1.137447	5782.43	295.61512	Fine
7	1661.8	403.3	4.1	0.320	0.339	0.019	1.18	0.000332	28.670	58.8	0.035383	97,713.84	1685.8063	Medium
8	1115.9	171.9	6.5	0.258	0.267	0.009	1.32	0.000146	12.620	105.3	0.094363	117,504.3	1328.856	Medium
9	1721.4	321.6	5.4	0.277	0.295	0.018	1.26	0.00019	16.450	55.2	0.032067	95,021.28	908.02962	Medium
10	750.3	140.5	5.3	0.281	0.296	0.015	1.26	0.000201	17.364	68.2	0.090897	51,170.46	1184.2511	Medium
11	735.5	134.9	5.5	0.283	0.293	0.010	1.26	0.000206	17.837	87.7	0.119239	64,503.35	1564.2956	Medium
12	1362.2	309.8	4.4	0.326	0.328	0.002	1.20	0.000357	30.855	38.9	0.028557	52,989.58	1200.2752	Gravelly
13	197.7	27.9	7.1	0.237	0.255	0.018	1.34	0.000107	9.2511	57.9	0.292868	11,446.83	535.63969	Medium
14	1259.2	90.7	13.7	0.171	0.179	0.008	1.58	3.41E-05	2.9434	83.0	0.065915	104,513.6	244.31807	Fine-medium
Men	862.9	1605	6.2	0.282	0.294	-	1.32	0.00024	20.736	77.1	0.23997	60,766.1	1652.996	
Range	71.3–1945.6	5.7–403.3	3.6–13.7	0.171–0.344	0.179–0.365	-	1.14–1.76	3.41E-05–0.00044	2.945–38.016	38.9–170.4	0.0285–1.13744	5782.43–13,2495.4	244.318–5722.01	

shows bulk resistivity values ranging from 71.9 to 4023.3 Ω m with mean value of 653.4 Ω m. The second layer has mean resistivity of 790.8 Ω m and a range of 71.3–2510.2 Ω m. The third inferred layer has resistivity range of 52.6–3428.8 Ω m. The fourth inferred layer gave an average resistivity value of 941.4 Ω m and a range of 46.1–2585.3 Ω m. The thickness of the topmost layer ranges from 0.5 to 11.3 m with average of 4.2 m. The second layer ranges in thickness between 1.6 and 170.4 m with average of 49.4 m. In layer three, the thickness ranges from 19.8 to 105.3 m with average of 55.8 m. The depth range and average remain the same as that of the thickness in the first layer while depth of the second layer ranges from 2.1 to 181.7 m with average of 53.2 m. The third layer has minimum depth of 41.0 m and maximum depth of 115.6 m, and its average depth is 71.3 m.

The estimation of aquifer geohydrodynamic parameters was done using the combinations of primary geoelectric parameters of aquifers determined from aquifer geoelectric samples and water samples through laboratory analysis. These parameters include aquifer water formation resistivity (ρ_w), aquifer formation factor (F), porosity (ϕ), tortuosity (τ), hydraulic conductivity or coefficient of permeability (K), Dar-Zarrouk parameters [transverse resistance (T) and longitudinal conductance (S)] as shown in Table 2. These parameters apart from aquifer porosity and water resistivity were derived from primary parameters and are referred to as secondary parameters (George et al. 2017b). The aquifer water resistivity (ρ_w) ranges from 5.7 to 403.3 Ω m with average of 160.50 Ω m. The aquifer formation factor F ranges from 3.6 to 13.7 with average of 6.2. The aquifer fractional porosity estimated from laboratory (ϕ_{lab}) ranged from 0.171 to 0.344, and the average was 0.288. Hydraulic conductivity (K) ranges from 2.943 to 38.016 m/day with average of 20.736 m/day. For accuracy in measurement, estimated porosity (ϕ_{cal}) was also determined using Archie's laws and values ranged from 0.179 to 0.365 with average of 0.294. The residuals between ϕ_{lab} and ϕ_{cal} are tolerable, and they are shown in Table 2. The estimated tortuosity ranged from 1.14 to 1.76 with average of 1.32.

The area has topographic elevations ranging from of 10 to 20 m with mean of 13.43 m. The maximum elevation (20 m) was obtained at Ikot Imo, while the minimum elevation (10 m) was lo-

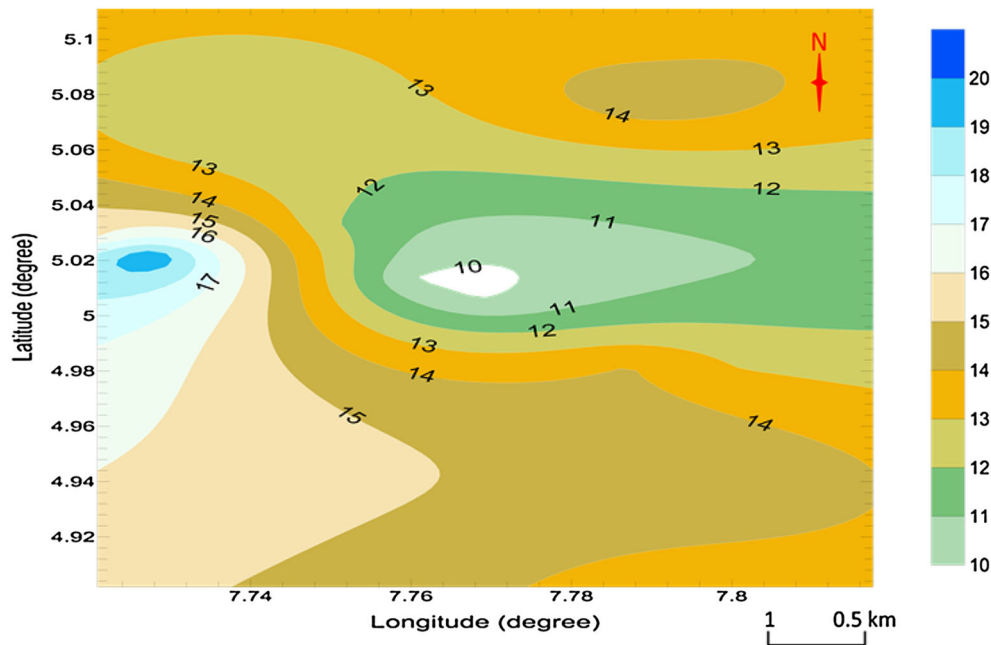


Figure 4. Contour map showing elevation distribution.

cated at Ikot Ekang (Fig. 4). In essence, the measured values actually show that the study area is low lying with moderately high elevation observed in the southwestern zone of the mapped area. The lowest elevation seems to be located at the central portion between northeast and southeast of the mapped area. The area has low water table, which makes the bearing pressure of the foundation layer to be low. The effect is mostly seen at the shorelines that are constantly eroded by the strong water current of the rivers.

The bulk aquifer resistivity, which was determined through electrical resistivity technique, is contoured in Figure 5. From the diagram, the bulk aquifer resistivity shows high values in the northwestern, central and the southwestern zones of the mapped area. The area with high bulk resistivity is likely to have economical water repositories as they are likely going to be saturated with pore water. If the water is not exposed to surface contamination, clean groundwater could be accessed in these zones of higher resistivity.

Pore water resistivity of aquifer, which was measured directly by water resistivity meter, was also contoured (Fig. 6). The distribution of water resistivity is similar to bulk aquifer resistivity. Specifically, highest values are found in the north-

western and central zones of the area. High values of bulk and water resistivities indicate both low conductivity and salinity of water in the area. The contour map in Figure 6 and the plot in Figure 7 show that aquifer bulk resistivity increases as water resistivity increases according to Eq. 10, which have high value of coefficient of determination of 0.829.

$$\rho_b = 0.1814\rho_w + 3.94 \quad (10)$$

The observed scatter in the plot is due to the heterogeneous nature of the formation in the coastal area studied. This inequality in the formation is responsible for uneven waterborne susceptibility of the formation to weathering and erosion at the shorelines where these geologic units are exposed. In the study area, the shorelines are often deteriorated by erosion and waterborne weathering, which affect the tarred road. The nature and distribution of geohydrodynamic parameters in both the vertical and horizontal segments of the subsurface and the low water table obtainable from the VES curves and logged boreholes reflect that the coastal shorelines are prone to erosion by water current.

The aquifer estimated formation factor (the ratio of bulk resistivity to water resistivity) in Figure 8 shows inversion in their distributions when

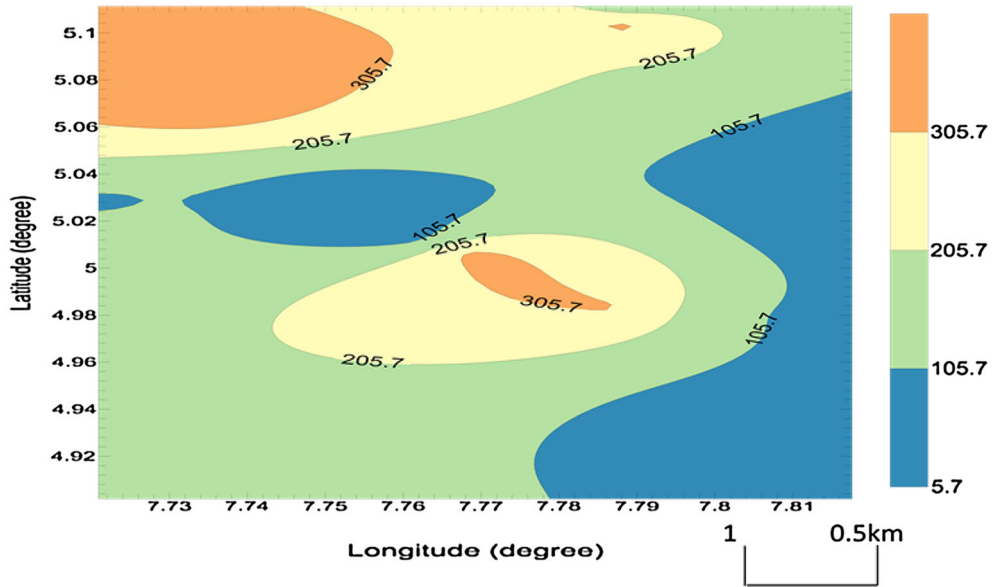


Figure 5. Contour map showing aquifer resistivity distribution.

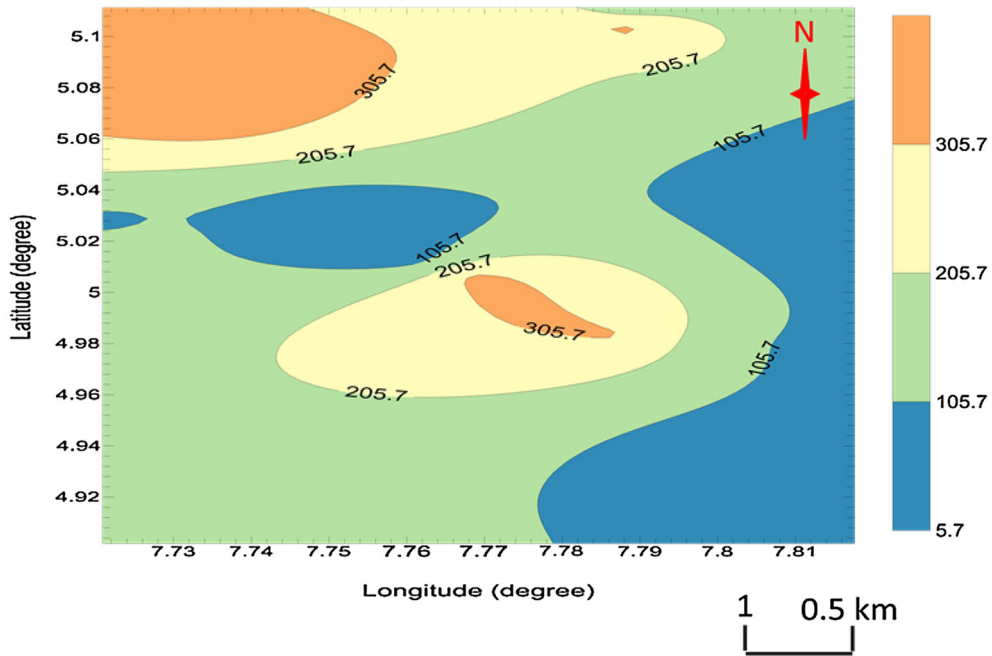


Figure 6. Contour map showing aquifer water resistivity distribution.

compared to the resistivity distribution. The north-eastern sector shows lower values of F while the northwestern and the southern regions have higher

values of formation factor. This implies that high bulk resistivity increases the water resistivity thereby reducing the formation factor.

The formation factor is an essential geological formation parameter that is used in estimating the porosity of the aquifer microstructure. It is also useful in estimating the cementation factor and the pore geometry factor. The formation resistivity factor displayed in contour map of Figure 8 shows increase in magnitude at locations where porosity decreases as shown in Figure 9a and b. This reflects the inverse relationship between porosity of arenaceous hydro-geounits and formation resistivity factor. This can be attributed to the high argillite-

sand mixing ratio that reduces pore-matrix ratios in aquifers. Tortuosity also increases as the formation factor increase (Fig. 10). This implies that argillites present in the fine-coarse sequence of sands hinder the rate of flow of water when comparing the macroscopic flow path length between the water/fluid inlet and outlet. The porosity values were measured using wet-weight dry-weight method discussed in the methodology. In all, the calculated porosity φ_{cal} obtained using average values of m and a estimated by George et al. (2015a) conforms very well to the laboratory-measured porosity φ_{lab} values, though φ_{cal} is slightly higher than φ_{lab} in all the stations (Table 2 for the residual values between φ_{cal} and φ_{lab}). The slightly higher values of φ_{cal} compared to φ_{lab} may be due to the failure of the aquifer sands to be completely clay free and completely saturated. The conformity between φ_{cal} and φ_{lab} can also be observed in the contour maps in Figure 9a and b. The hydraulic conductivity, K , which is connected (Fig. 11) to porosity φ_{lab} was estimated using the Kozeny-Carman-Bear's equation (Eq. 6). The contour map of estimated values of K in m/day shows a steady decrease in K from east to west of the study area. Although the values show that the area is mainly trending in a predictable manner, the minor inversion in value of K in some locations may indicate the presence of pockets of

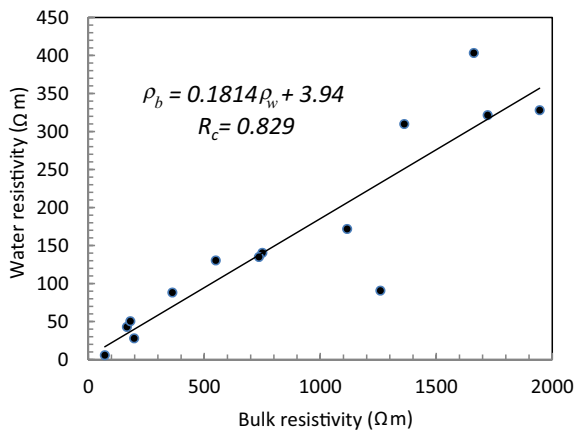


Figure 7. Aquifer water resistivity against bulk aquifer resistivity.

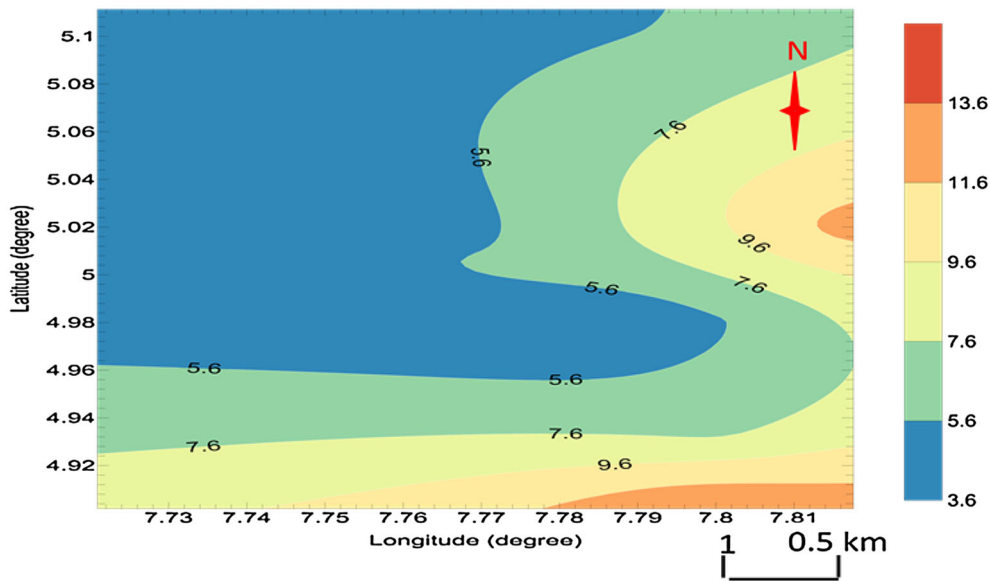


Figure 8. Aquifer formation factor distribution.

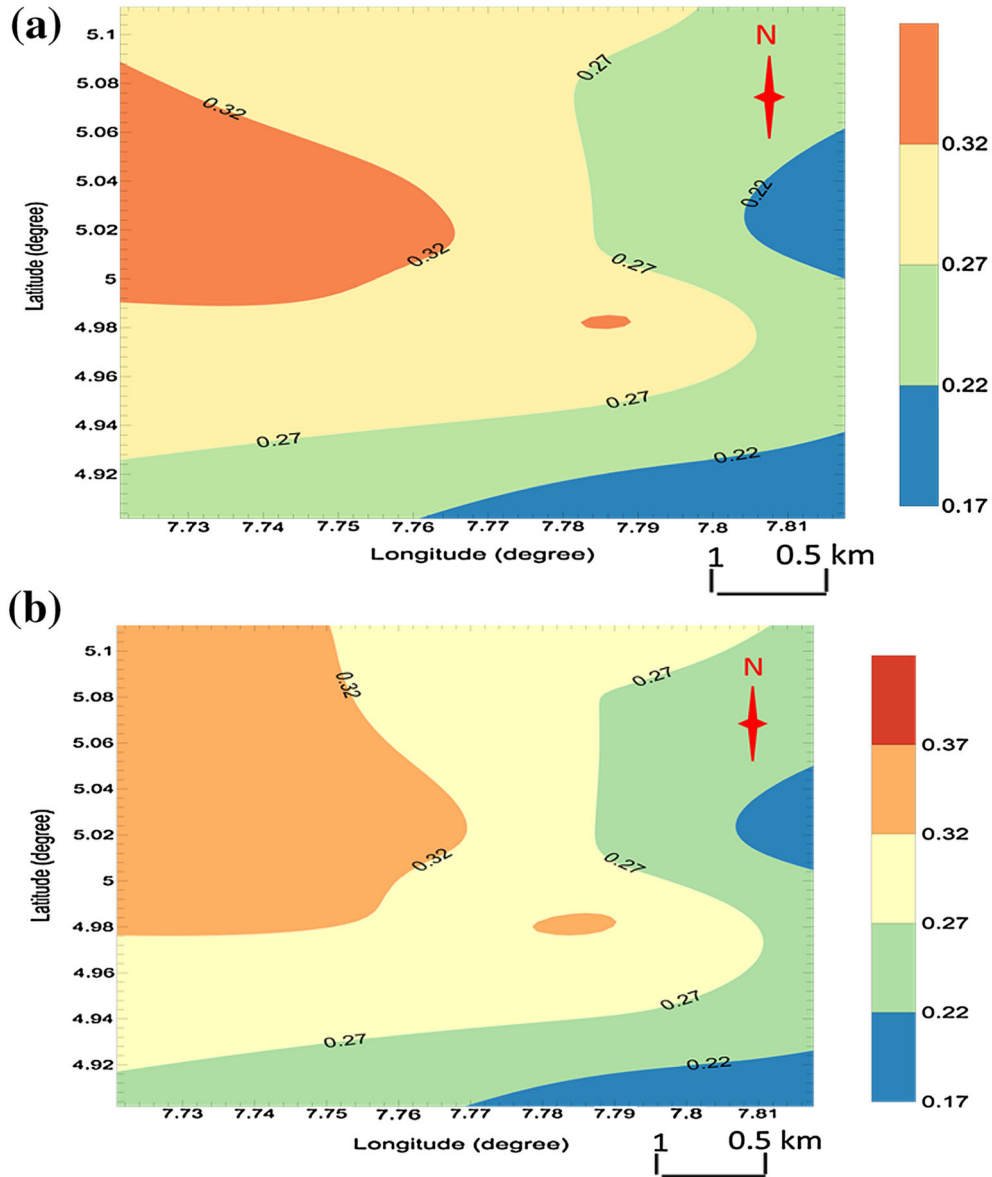


Figure 9. (a) Aquifer porosity (ϕ_{lab}) distribution obtained from laboratory analysis. (b) Aquifer porosity (ϕ_{cal}) distribution obtained from laboratory analysis.

argillaceous materials in the aquifer repositories *vis-a-vis* other units in the geological sequence. Unlike F , the coefficient of permeability, K shows an exponential increase with ϕ_{lab} in the regression analysis (Fig. 12). This is symptomatic of the fact that hydraulic conductivity increases as porosity increases as evidenced by the high coefficient of determination (0.9993).

The regressed function in Eq. 11 gives the K - ϕ_{lab} relation of the aquifer geologic units in the coastal formation.

$$K = 1880.6\phi_{lab}^{3.4749} \quad (11)$$

This power law can be used to estimate the hydraulic conductivity of the coastal formation once the ϕ_{lab} or the ϕ_{cal} is available.

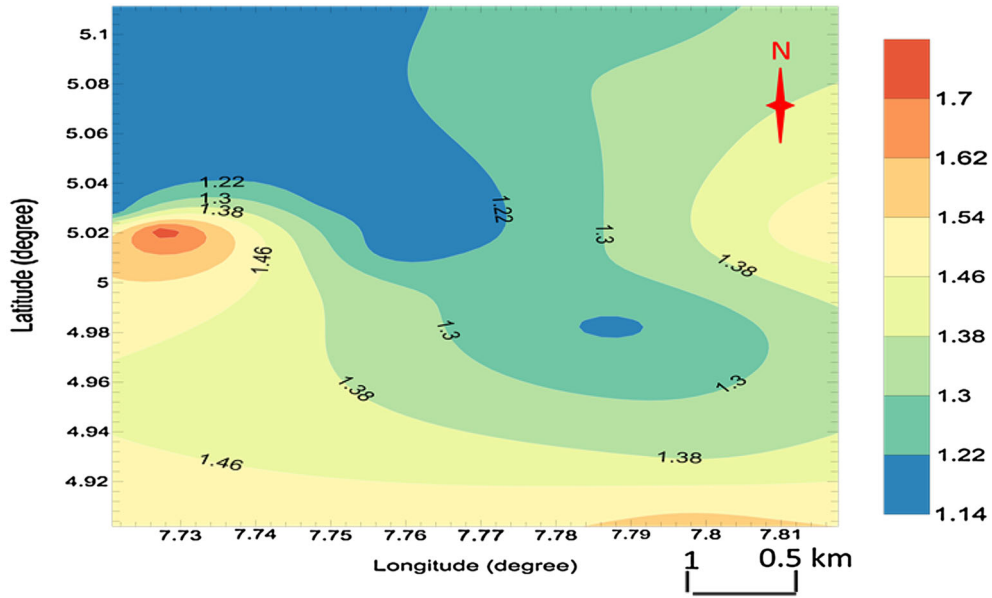


Figure 10. Distribution of estimated aquifer tortuosity (τ).

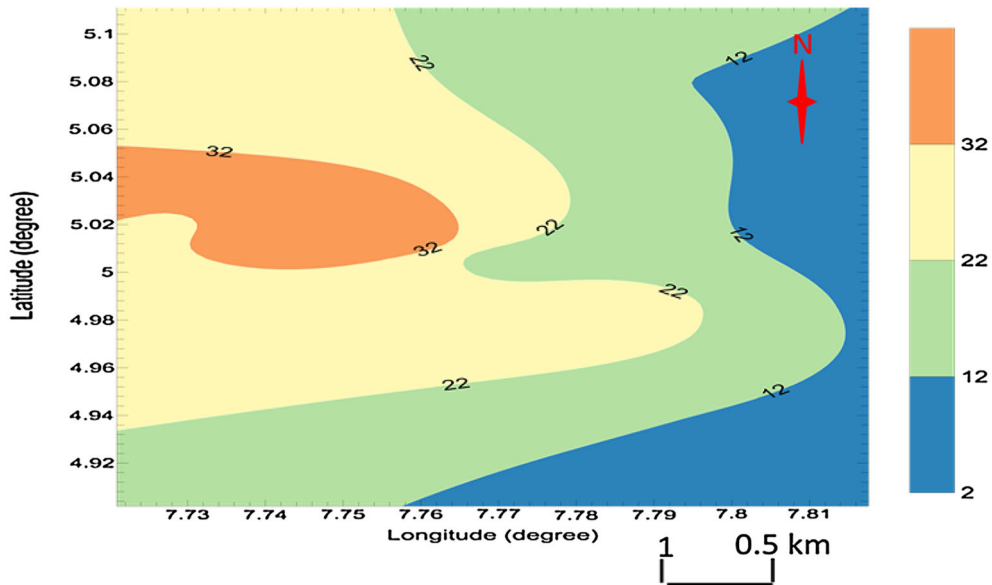


Figure 11. Distribution of estimated coefficient of permeability (hydraulic conductivity).

Using the primary aquifer repository parameters [thickness (h) and bulk resistivity (ρ_b)], the Dar-Zarrauk parameters [transverse resistance (T) and longitudinal conductance (S)] were estimated. The aquifer thickness varies in the study area (Fig. 13);

low thicknesses are found in the northwestern and southeastern regions of the mapped area. The area seems to have prolific shallow aquifers because the mapped region has thickness that is greater than 40 m in all the sampled points.

The transmissivity (Tr) estimated as product of K and h in (m²/day) was computed from processed VES data. The observed high values of Tr (Table 2) equally attest to the prolificacy of the aquifer repositories (George et al. 2018). The computed Tr was contoured and the spatial distribution shows the least values on the average occupying the western region of the study area while larger values occupy the eastern region (Fig. 14). This distribution pattern gives an insight to the prediction of the pore geofluid flow in the area. In terms of Dar-Zarrouk

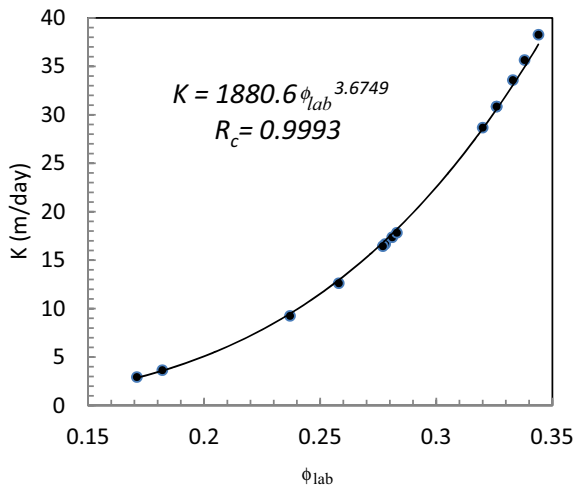


Figure 12. Aquifer K vs. ϕ_{lab} in the study area.

parameters, the transverse resistance T in Ω m² and longitudinal conductance S in Ω^{-1} (Siemens) were estimated. The contours of T and S are displayed in Figures 15 and 16, respectively. Transverse resistance shows some seemingly low values $T \leq 50,000$ Ω m² mid-way between the western and eastern parts of the mapped area (Fig. 15). In all, the estimated T values show that the exploited aquifer repositories are prolific but open to surface contamination due to low longitudinal conductance generally less than 1 Siemens in Figure 16 (Oladapo et al. 2004; George et al. 2016). The Dar-Zarrouk parameters (T and S) show inverse relation (Fig. 17). The heterogeneous and large variations in particle size are responsible for low value of coefficient of determination (0.527) in the regressed plot between T and S . However, the power law equation gives the relation between T and S :

$$T = 10111S^{-0.673} \tag{12}$$

Characteristically, the delineated aquifers appear to have generally low salinity due to low conductivity/high resistivity and high flow rate in regions characterized by well-sorted sands. Besides, the aquifers, though generally having longitudinal conductance that is less than unity and hence not protected from contaminations, are well exploited in the study area because of their accessibility as characterized by low water table seen in this work as well as prolificacy characterized by high transverse resistance. The

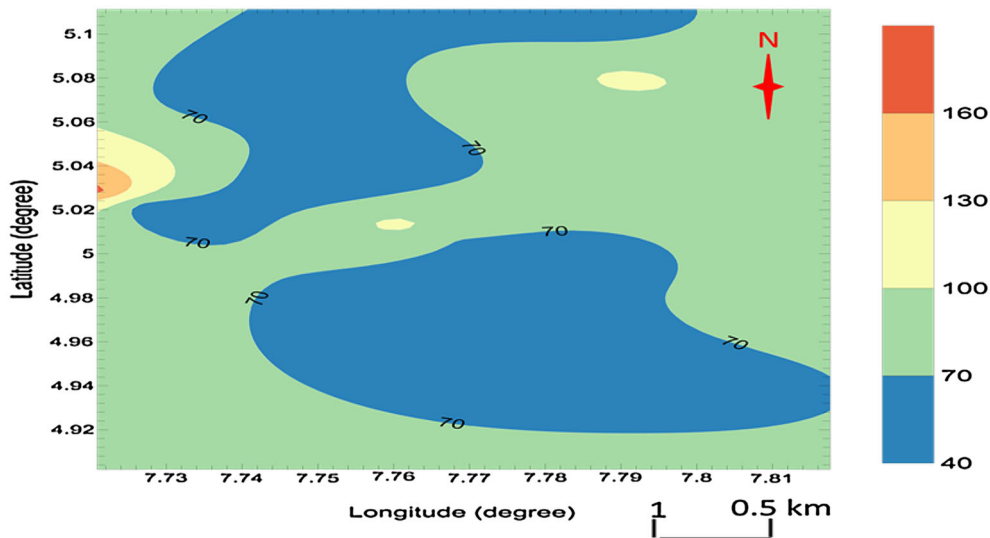


Figure 13. Distribution of estimated aquifer thickness.

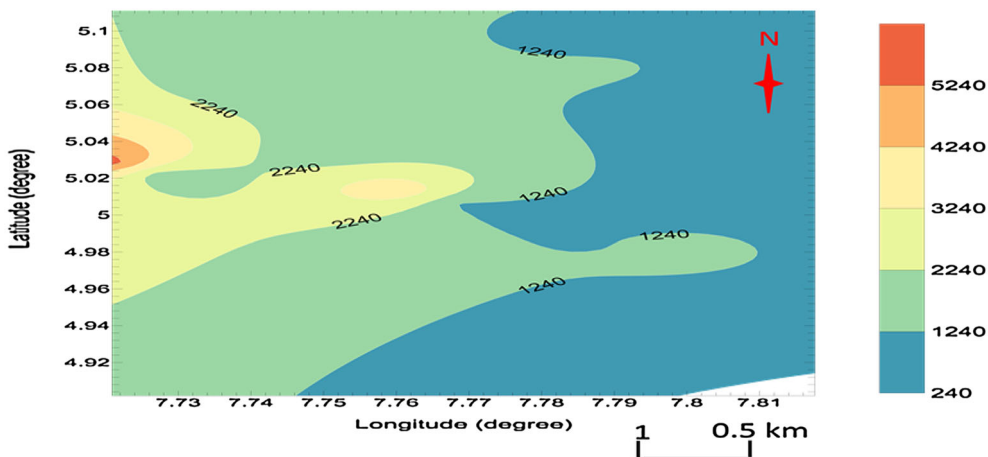


Figure 14. Distribution of estimated aquifer transmissivity.

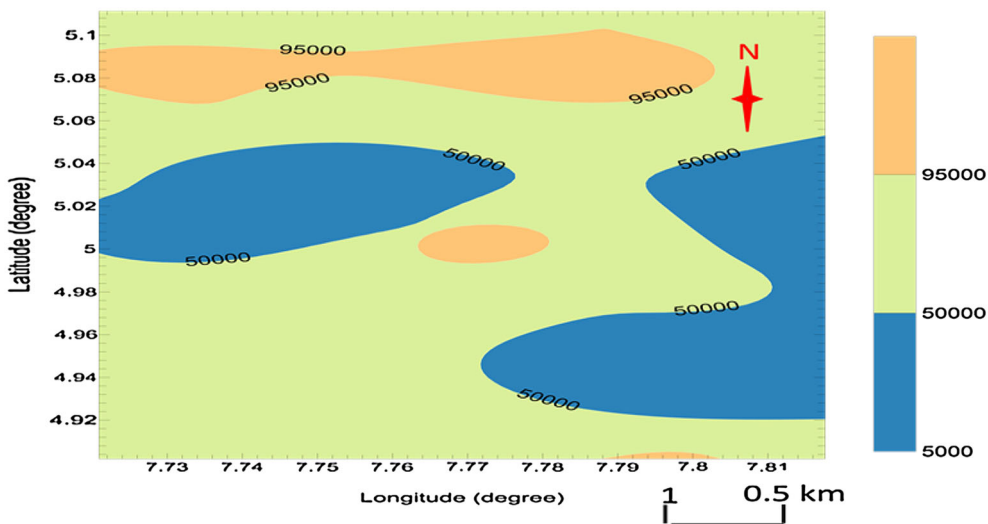


Figure 15. Distribution of estimated aquifer transverse resistance.

estimated Dar-Zarrouk parameters may be useful in the modeling of the contaminant plume and estimation of corrosivity of the exploited water repositories.

CONCLUSIONS

The results of VES and complementary laboratory technique aided by hydrogeological information have been used to characterize hydrogeological repositories in terms of hydrodynamic parameters in

the Abak Local Government Area, the coastal region of Nigeria with erosion-prone vulnerable shorelines. The combination of the resistivity exploratory technique and the complementary laboratory method in company with the geological and borehole lithologic information permitted the extrapolation of geoelectric and geohydrodynamic parameters (Tables 1 and 2). The determination of coefficient of permeability using geophysical measurement and laboratory analysis in combination with semiempirical equations of petrophysics and fractional porosity measured from geophysical and

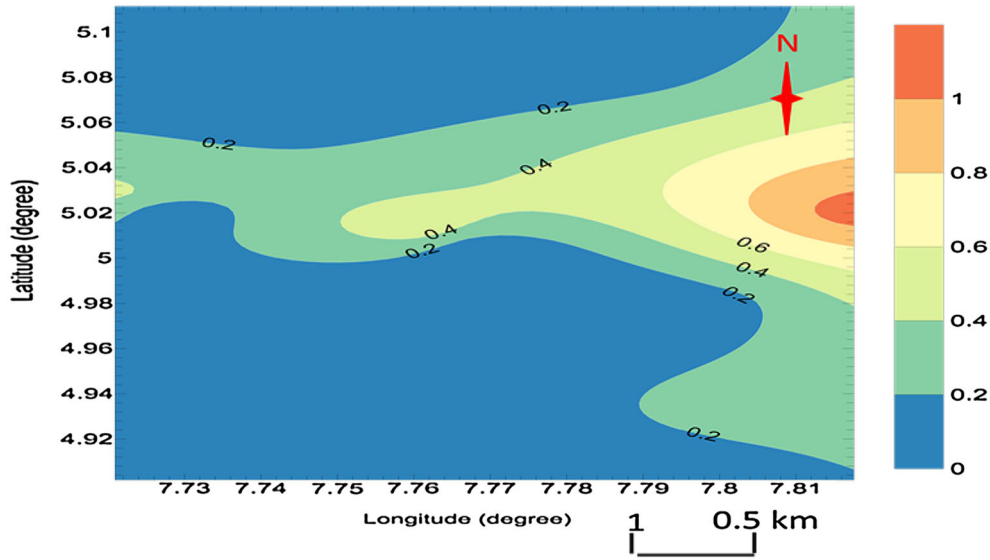


Figure 16. Distribution of estimated aquifer longitudinal conductance.

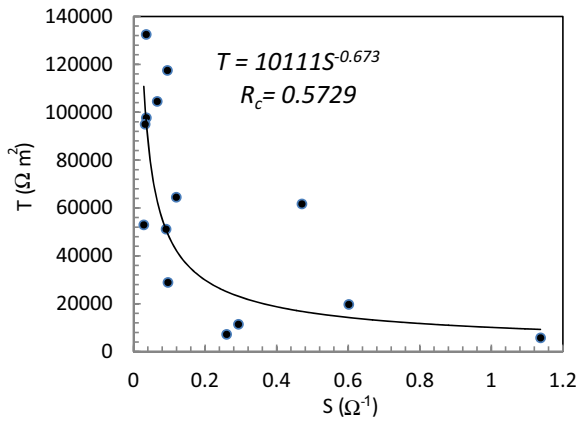


Figure 17. Aquifer T vs. S in the study area.

laboratory technique is useful in the study of subsurface microstructure and groundwater flow and contamination study. The geohydrodynamic parameters serve as primary source of information for the study of the deeper geologic units. These parameters are essential elements that are paramount in groundwater resource management and conservation as well as serving as guide to checking the waterborne erosion in the shorelines. This is already possible because the constant collapse of the Abak River shoreline is attributed to the highly porous and permeable geologic stratigraphic se-

quence of both the saturated and unsaturated formations penetrated by current which are all exposed to degrading water current in the area. The parameters that are responsible for formation stability are the inter-related geoelectric-geohydraulic parameters primarily used in qualitative and quantitative characterization of geologic and hydrogeologic sediments. The evaluated ranges of parameters of groundwater repository in the survey are wide as a result of increased inhomogeneity of arenaceous geological water repositories. The formation electrohydraulic models and their contours for the superficially assessable water beds can enhance a better understanding of the geohydrodynamics of survey area. To improve the quality of models in the study area, the generated maps and mathematical models are essential prerequisites for mapping the contaminant plumes in the groundwater repositories. The results can also serve as reference study that guarantees quality assurance in similar and related studies undertaken within the area.

ACKNOWLEDGMENTS

We are grateful to the reviewers' and the editor's comments, which have helped us improve the quality of this manuscript.

FUNDING

Funding was provided by Akwa Ibom State University.

REFERENCES

- Aguilera, R. (1976). Analysis of naturally fractured reservoirs from conventional well logs. *Journal of Petroleum Technology*, 28, 764–772.
- Akpan, A. E., George, N. J., & George, A. M. (2009). Geophysical investigation of some prominent gully erosion sites in Calabar, South-Eastern Nigeria and its implications to hazard prevention. *Disaster Advances*, 2(3), 46–50.
- American Petroleum Institute, API. (1960). Recommended practice for core analysis procedure. Report No. 40 (p. 55).
- Archie, G. E. (1942). The electrical resistivity log as an aid in determining some reservoirs characteristic grain. *AIME*, 146, 54–62.
- Atkins, E. R., Jr., & Smith, G. H. (1961). The significance of particle shape in formation factor—Porosity relationship. *Journal of Petroleum Technology*, 13, 285–291.
- Batayneh, A. T. (2009). A hydroeophysical model of the relationship between geoelectric and hydraulic parameters, Central Jordan. *Journal of Water Resource and Protection*, 1, 400–407.
- Bear, J. (1972). *Dynamics of fluids in porous media*. New York: Elsevier.
- Bhattacharya, P. K., & Petra, H. P. (1968). *Direct current geoelectric sounding: Principles and interpretation*. Amsterdam: Elsevier.
- Carman, P. C. (1937). Fluid flow through granular beds. *Transactions of the Institute of Chemical Engineers*, 15, 150–156.
- Carman, P. C. (1938). The determination of the specific surface of pocoders I. *Journal of the Society of Chemical Industrialists*, 57, 225–234.
- Carman, P. C. (1956). *Flow of gases through porous media* (p. 182). London: Butterworths.
- Chakravarthi, V., Shankar, G. B. K., Murahidharan, D., Hari-narayana, T., & Sundararajan, N. (2007). An integrated geophysical approach for imaging sub basalt sedimentary basins: Case study of Jam River Basin, India. *Geophysics*, 72(6), B141–B147.
- Ehrlich, R., Etris, E. L., Brumfield, D., Tuan, L. P., & Crabtree, S. J. (1991). Petrography and reservoir physics. Part 111: Physical models for permeability and formation factor. *Bulletin of the American Association of Petroleum Geologists*, 75, 1579–1592.
- Emerson, D. W. (1969). Laboratory electrical resistivity measurement of rocks. *Proceedings of the Australasian Institute of Mining and Metallurgy*, 230, 51–62.
- Evans, U. F., George, N. J., Akpan, A. E., Obot, I. B., & Ikot, A. N. (2010). A study of superficial sediments and aquifers in parts of Uyo Local Government area, Akwa Ibom State, Southern Nigeria, using electrical sounding method. *India. E-Journal of Chemistry*, 7(3), 1018–1022.
- Faris, S. R., Gournay, L. S., Lipson, L. B., & Webb, T. S. (1954). Verification of tortuosity equations. *Bulletin of the American Association of Petroleum Geologists*, 38, 2226–2232.
- Fetters, C. W. (1994). *Applied hydrology* (3rd ed.). Upper Saddle River: Prentice-Hall.
- Folk, R. L. (1966). A review of grain-size parameters. *Sediment*, 6, 73–93.
- Galehouse, J. S. (1971). Sedimentation analysis. In R. F. Carver (Ed.), *Procedures in sedimentary petrology*. New York: Wiley.
- George, N. J. (2006). Resistivity study of shallow aquifers at Southern Ukanafun L. G. A., Akwa Ibom State. Unpublished Master's Thesis, Department of Physics, University of Calabar, Calabar, Nigeria.
- George, N. J. A., Akpan, A. E., & Ekanem, A. M. (2016). Assessment of textural variational pattern and electrical conduction of economic and accessible quaternary hydroolithofacies via geoelectric and laboratory methods in SE Nigeria: A case study of select locations in Akwa Ibom State. *Journal of Geological Society of India*, 88(4), 517–528.
- George, N. J., Atat, J. G., Udoinyang, I. E., Akpan, A. E., & George, A. M. (2017a). Geophysical assessment of vulnerability of surficial aquifer: A case study of oil producing localities and Riverine areas in the coastal region of Akwa Ibom state, southern Nigeria. *Current Science*, 113(3), 430.
- George, N. J., Ekanem, A. M., Ibang, J. I., & Udosen, N. I. (2017b). Hydrodynamic Implications of Aquifer Quality Index (AQI) and Flow Zone Indicator (FZI) in groundwater abstraction: A case study of coastal hydroolithofacies in South-eastern Nigeria. *Journal of Coastal Conservation*, 21(6), 759–776. <https://doi.org/10.1007/s11852-017-0535-3>.
- George, N. J., Ekong, U. F., & Etuk, S. E. (2014). Assessment of economically accessible groundwater reserve and its protective capacity in Eastern Obolo Local Government Area of Akwa Ibom State, Nigeria, using electrical resistivity method. *ISRN Geophysics*. <https://doi.org/10.1155/2014/578981>.
- George, N. J., Emah, J. B., & Ekong, U. N. (2015a). Geohydrodynamic properties of hydrogeological units in parts of Niger Delta, southern Nigeria. *Journal of African Earth Sciences*, 105, 55–63. <https://doi.org/10.1016/j.jafrearsci.2015.02.009>.
- George, N. J., Ibuot, J. C., Ekanem, A. M., & George, A. M. (2018). Estimating the indices of inter-transmissibility magnitude of active surficial hydrogeologic units in Itu, Akwa Ibom State, southern Nigeria. *Arabian Journal of Geosciences*, 11(6), 1–16. <https://doi.org/10.1007/s12517-018-3475-9>.
- George, N. J., Ibuot, J. C., & Obiora, D. N. (2015b). Geoelectrohydraulic parameters of shallow sandy aquifer in Itu, Akwa Ibom State (Nigeria) using geoelectric and hydrogeological measurements. *Journal of African Earth Sciences*, 110, 52–63. <https://doi.org/10.1016/j.jafrearsci.2015.06.006>.
- George, N. J., Obianwu, V. I., Akpan, A. E., & Obot, I. B. (2010). Assessment of shallow aquiferous units and coefficients of anisotropy in the coastal plain sand of southern Ukanafun Local Government Area, Akwa Ibom state, Southern Nigeria. *Scholars Research Library*, 1(2), 118–128.
- Gowd, S. S. (2004). Electrical resistivity surveys to delineate groundwater potential aquifers in Peddavanka watershed, Anantapur district, Andhra Pradesh, India. *Environmental Geology*, 46, 118–131.
- Gratan, L. C., & Fraser, H. J. (1935). Systematic packing of sphere with particular relation to porosity and permeability. *The Journal of Geology*, 34, 785–909.
- Gurunadha Roa, V. V. S., Tamma Roa, G., Surinaidu, L., Rajesh, R., & Mahesh, J. (2011). Geophysical and geochemical approach for seawater intrusion assessment in the Gadavari Delta Basin, A. P. India. *Water, Air, and Soil Pollution*, 217, 503–514.
- Ibang, J. I., & George, N. J. (2016). Estimating geohydraulic parameters, protective strength, and corrosivity of hydrogeological units: A case study of ALSCON, Ikot Abasi, southern Nigeria. *Arabian Journal of Geosciences*, 9(5), 1–16. <https://doi.org/10.1007/s12517-016-2390-1>.

- Ibuot, J. C., Akpabio, G. T., & George, N. J. (2013). A survey of the repository of groundwater potential and distribution using geoelectrical resistivity method in Itu Local Government Area, Akwa Ibom State, Southern Nigeria. *Central European Journal of Geosciences*, 5(4), 538–547.
- Igboekwe, M. U., Prakash, B. A., Yadaih, P., Kuma, K. M., & Chandrasekhar, S. B. N. (2004). Groundwater Potentials in Abia State, Nigeria. A report submitted to the National Geophysical Research Institute, Hyderabad, India.
- Keller, G. V. (1982). Electrical properties rocks and minerals. In R. S. Carmichael (Ed.), *Handbook of physical properties of rock* (Vol. 1, pp. 217–293). Boca Raton: CRC Press.
- Keller, G. V., & Frischknecht, F. C. (1966). *Electrical methods in geophysical prospecting* (p. 517). London: Pergamon.
- Kezdi, A. (1974). *Handbook of soil mechanism* (p. 294). Amsterdam: Elsevier.
- Kogbe, C. A. (1989). *Geology of Nigeria*. Jos: Rock View Nigeria Limited.
- Mbipom, E. W., Okwueze, E. O., & Onwuegbuche, A. A. (1996). Estimation of transmissivity using VES data from the Mbaise Area of Nigeria. *Nigerian Journal of Physics*, 85, 28–32.
- Obianwu, V. I., George, N. J., & Udofia, K. M. (2011). Estimation of aquifer hydraulic conductivity and effective porosity distributions using laboratory measurements on core sample in the Niger Delta, southern Nigeria. *International Review Physics Praise Worthy Prize, Italy*, 5(1), 19–24.
- Oladapo, M. I., Mohammed, M. Z., Adeoye, O. O., & Adetola, O. O. (2004). Geoelectric investigation of the Ondo State Housing Corporation Estate; Ijapo, Akure, southwestern Nigeria. *Journal of Mining and Geology*, 40(1), 41–48.
- Orellana, E., & Mooney, H. (1966). *Master tables and curves for VES over layered structures*. Madrid: Interciencia.
- Owen, J. E. (1952). The resistivity of a fluid filled porous body. *Transactions of the AIME*, 195, 169–174.
- Pettijohn, F. J., & Potter, P. (1972). *Sand and sandstone. "Porosity and permeability"*. Berlin: Springer.
- Towel, G. H. (1962). An analysis of the formation resistivity factor—Porosity relationship of some assumed pore geometries. In *Transactions SPWLA, 3rd annual logging symposium* (pp. ccl-13). May 17–18, Huston, Texas.
- Vanovermehren, R. A. (1989). Aquifer boundaries explored by geoelectrical measurement of Yemen: A case of equivalence. *Geophysics*, 54, 38–48.
- Winsauer, W. O., Shearin, H. M., Masson, P. H., & Williams, M. (1952). Resistivity of brine saturated sands in relation to pore geometry. *Bulletin of the American Association of Petroleum Geologists*, 36, 253–277.
- Wyllie, M. R., & Gregory, A. R. (1953). Formation factors of unconsolidated porous media. Influence of particle shape and effect of cementation. *Transactions of the AIME*, 198, 103–110.
- Wyllie, M. R. J., & Rose, W. D. (1950). Some theoretical consideration related to the quantitative evaluation of the physical characteristics of reservoir rocks from electrical log data. *Transactions of the AIME*, 189, 105–118.
- Zohdy, A. A. R. (1965). The auxiliary point method of electrical sounding interpretation and its relations to the Dar-Zarrouk parameters. *Geophysics*, 30, 644–660.
- Zohdy, A. A. R., Eaton, G. P., & Mabey, D. R. (1974). Application of surface geophysics to groundwater investigation. USGS techniques of water resources investigations book 2 chapter DI (p. 116).